Multi-model finite element approach for stress analysis of composite laminates

U.N. Band[1] and *†Y.M. Desai[2]
[1,2]Civil Engineering Department, Indian Institute of Technology Bombay, Mumbai, India.

*Presenting author: desai@civil.iitb.ac.in
†Corresponding author: desai@civil.iitb.ac.in

Abstract

A multi-model global-local approach to study free edge effects in laminated composites subjected to uniaxial in-plane loads is presented in this paper. Mixed layer-wise (LW) finite element (FE) model is used in critical free edge zone. Remaining part of plate is modelled by using higher order equivalent single layer (ESL) theory. A transition element is developed to ensure a compatibility between differently modelled subdomains. This combined model possesses traits of both ESL and LW mixed models. Higher order ESL predicts global parameters efficiently, on the other hand, mixed LW model captures the interlaminar stresses at local zones. Mixed LW model includes the transverse stresses as nodal degrees of freedom (DOF) ensuring continuity of the transverse stresses over layer interfaces without using any additional stress functions. Both, ESL and LW mixed models are developed by using three dimensional (3D) elasticity relationships and principle of minimum potential energy. The present combined model is a good blend of computational efficiency and accuracy in prediction of local transverse stresses. Plates with different stacking sequences are investigated for free edge stresses developed in the transverse direction under uniaxial in-plane load conditions.

Key Words: Mixed Finite Element; Free edge stresses; Higher order theory; Principle of minimum potential energy; transition element; global-local analysis.

1.0 Introduction

Laminated composites having several layers with uni-directional fibres are utilized as structural members for variety of applications. Advantageously, these exhibit good strength, stiffness, environmental resistance and are light in weight as compared to homogeneous materials. Depending on configuration of loading, strength parameters can be altered by using appropriate stacking sequence of layers. Evaluation of laminate response to applied load becomes complex due to heterogeneous properties of different layers in a laminate.

Apart from elasticity approach, various displacement based and hybrid models have been proposed for analysis of laminates. These models are implemented using analytical or FE formulations. A three-dimensional (3D) elasticity solution by Pipes and Pagano (1970) [1] has shown that in a laminate under simple uniaxial loading there is a "*boundary layer*" region along the free edges where a three-dimensional state of stress exists, and that the boundary layer thickness is roughly equal to laminate thickness. Wang and Crossman (1977) [2] presented a displacement based FE model to study edge effects for symmetrically stacked laminates. It has been shown that steep stress gradients of the transverse normal and shear stresses prevail near free edges. These high magnitudes of multi-axial stresses in vicinity of free edges may lead to delamination of a laminate. A state of plane stress is seen to prevail towards the interior of plate. Moreover, delamination failure is most common mode of failure in laminated composites, which initiates at geometrical discontinuities like free edges, notches and holes.

Evidently, a correct evaluation of complete 3D state of stress at free edges is important for assessment of strength and durability of a laminate under a certain load configuration. Effect of stacking sequence on laminate strength was investigated by Pagano and Pipes (1971) [3]. Rybicki (1971) [4], Wu and Hsu (1993) [5], Flesher and Herakovich (2006) [6] presented different approaches for evaluation of the transverse stresses and prediction of onset of delamination. Shi and Chen (1992) [7]presented a mixed FE model by using a hybrid stress element at free edges and conventional displacement based FE's at other locations. Chorng-Fuh and Horng-Shian (1993) [8] also presented a mixed FE model to predict the transverse stresses developed at free edges of a laminate subjected to uniform in-plane strain

A displacement model depicting the kinematics of a particle in a laminate must encompass rigid body, extension, bending and warping modes of deformation to correctly predict response in a realistic manner. Many ESL models are seen in literature for analysis of laminated composites. Kant and Swaminathan (2002) [9] presented a comprehensive ESL higher order theory which incorporates all these deformation modes and predicts all global responses effectively. Laminate is considered as a single smeared plate with the properties averaged over thickness. However, evaluation of interlaminar transverse stresses is done by using 3D stress equilibrium equations. On the other hand, a better mathematical representation of laminate behaviour is portrayed by LW models which incorporate discrete individual properties of all layers in a laminate. Displacement based LW models also need either some additional stress function or integration of stress equilibrium equations to estimate magnitudes and through thickness variation of the transverse stresses in a laminate. Ramtekkar, Desai (2002) [10] presented a FE mixed LW formulation having the transverse stresses invoked as nodal DOF along with displacements. Continuity of the transverse stresses over layer interfaces is inherently satisfied. ESL's demand less computational effort as compared to LW models as they map the domain involving less DOF. Computational efficiency is achieved by using ESL but accuracy of solution is sacrificed. LW models exhibit accuracy of solution but demand high computational effort. Application of LW models on a laminate domain involve high DOF in the solution and face restrictions due to limitation of computational resources in cases where fine discretization of domain becomes essential for accuracy of solution.

In this paper a multi-model meshing methodology is presented which advantageously uses both higher order ESL and mixed LW models simultaneously over the domain of a laminate. A transition element is developed to establish compatibility between two models. Presence of ESL in non-critical zones in a laminate ensures accurate assessment of global parameters and reduction of computational cost. At the same time, mixed LW model used in critical free edge region accurately predicts the transverse stresses. Efficacy of present multi-model approach is illustrated by using it on examples of laminates subjected to uniaxial in-plane loading.

2.0 Theoretical formulation

Three models have been formulated for analysis of laminated composite plates consisting of several orthotropic laminae.

(a) **Model 1**: This model adopts a cubic displacement field in the thickness direction for displacements (U,V,W) and has 12 DOF. The theory has been identified as HOST12. The model is based on the three dimensional state of stresses and strains.

(b) **Model 2**: In this model, mixed finite element LWT, which has three displacements (U,V,W) and the transverse stresses ($\tau_{xz}, \tau_{yz}, \sigma_z$) as the nodal DOF, is used. The theory is based on elasticity relationships. Therefore, introduction of any additional parameters/stress variation functions are advantageously avoided.

(c) **Model 3**: This model is based on a global-local finite element procedure to take advantage of computational efficiency of the higher order ESL theory and accuracy of the 3D mixed model.

2.1 Model 1 : Development of ESL theory based model (HOST 12)

Displacements in three principal directions of the laminate as a fully cubic function of the thickness co-ordinate are

$$\begin{aligned} u(x,y,z) &= u_0(x,y) + z\theta_x(x,y) + z^2 u_0^*(x,y) + z^3\theta_x^*(x,y) \\ v(x,y,z) &= v_0(x,y) + z\theta_y(x,y) + z^2 v_0^*(x,y) + z^3\theta_y^*(x,y) \\ w(x,y,z) &= w_0(x,y) + z\theta_z(x,y) + z^2 w_0^*(x,y) + z^3\theta_z^*(x,y) \end{aligned} \tag{1}$$

The above displacement field eliminates any requirement of shear correction factor and chances of shear locking. Here u_0, v_0 and w_0 are the deformations in the x,y,z (laminate co-ordinate) directions respectively at the mid-plane. θ_x, θ_y and θ_z, on the other hand, are the rotations at mid-plane about the principal directions of laminate. $u_0^*, \theta_x^*, v_0^*, \theta_y^*, w_0^*$ and θ_z^* are higher order terms stemming from the Taylor's series. By using material property, the strain displacement relationship and the principle of minimum potential energy, the stiffness matrix for laminate is developed. By using shape functions similar to the stiffness evaluation, the mass matrix is also developed. Detailed formulation can be seen in the work presented by Kant and Swaminathan (2002) [9]. A nine node Lagrangian isoparametric element has been used to discretize a laminate.

Numerical integration is performed by employing 3 X 3 Gauss quadrature rule for the extension, bending, mass component, whereas, 2 X 2 Gauss rule for the shear part.

2.2 Model 2: Development of mixed LW model

An 18-node three-dimensional element based on mixed formulation is used by considering displacement fields *u*(*x*,*y*,*z*), *v*(*x*,*y*,*z*) and *w*(*x*,*y*,*z*) having quadratic variation along the plane of plate and cubic variation in the transverse direction. The cubic variation of field has been adopted to invoke the transverse stresses as the nodal parameters in addition to the nodal deformations. The displacement field is expressed as

$$u_k(x,y,z) = \sum_{i=1}^{3}\sum_{j=1}^{3} g_i h_j a_{0ijk} + z\sum_{i=1}^{3}\sum_{j=1}^{3} g_i h_j a_{1ijk} + z^2\sum_{i=1}^{3}\sum_{J=1}^{3} g_i h_j a_{2ijk} + z^3\sum_{i=1}^{3}\sum_{j=1}^{3} g_i h_j a_{3ijk} \tag{2}$$

where

$$g_1 = \frac{\xi}{2}(\xi - 1),\ \ g_2 = 1 - \xi^2\ ,\ \ g_3 = \frac{\xi}{2}(1+\xi),\quad \xi = x/L_x$$

$$h_1 = \frac{\delta}{2}(\delta - 1),\ \ h_2 = 1 - \delta^2\ ,\ \ h_3 = \frac{\delta}{2}(1+\delta),\quad \delta = y/L_y$$

$$k = 1, 2, 3 \text{ and } u_1 = u; \quad u_2 = v; \quad u_3 = w;$$

Further, a_{mijk} ($m = 0, 1, 2, 3; i, j, k = 1, 2, 3$) are the generalized coordinates.

Variation of displacement fields has been assumed to be cubic through the thickness of element, although there are only two nodes along 'z' axis of an element. Derivative of displacement with respect to the thickness coordinate has also been included in the displacement field. Such a variation is required for invoking transverse stress components σ_z, τ_{xz} and τ_{yz} as nodal DOF in the present formulation. Further, it also ensures quadratic variation of the transverse stresses through the thickness of an element.

By making use of the elasticity relationship and introducing derivative of displacements, displacement field $u_k(x,y,z)$) in Eq. (2) becomes

$$u_k(x,y,z) = \sum_{n=1}^{18} g_i h_j (f_q u_{kn} + f_p \hat{u}_{kn}) \tag{3}$$

Here, $i = 1, 2, 3$ for the nodes with $\xi = -1$, $\xi = 0$ and $\xi = 1$, respectively;
$j = 1, 2, 3$ for the nodes with $\delta = -1$, $\delta = 0$ and $\delta = 1$, respectively;

$q = 1,2$ and $p = 3,4$ for the nodes with $\eta = -1$ and $\eta = 1$, respectively for node numbers 1 to 18 and

$$f_1 = \frac{1}{4}(2 - 3\eta + \eta^3);\ f_2 = \frac{1}{4}(2 + 3\eta - \eta^3);\ f_3 = \frac{L_z}{4}(1 - \eta - \eta^2 + \eta^3);\ f_4 = \frac{L_z}{4}(-1 - \eta + \eta^2 + \eta^3).$$

Here, f_3 and f_4 correspond to derivative of displacements with respect to thickness co-ordinate whereas f_1 and f_2 correspond to displacement DOF , u_{kn} ($k = 1, 2, 3$ and $n = 1,2,3,...18$) are nodal displacement variables, whereas $\hat{u}_{kn}$ $\left(= \frac{\partial u_{kn}}{\partial z}\right)$ contains the nodal transverse stress variables. Principle of minimum potential energy is used to develop the element property matrix. Detailed formulation can be seen in the work presented by Ramtekkar, Desai (2002) [10].

Numerical integration of system matrices has been performed by using Gauss quadrature rule with 3 X 3 integration scheme in plane of plate and a 5 X 5 integration scheme in the thickness direction.

2.3 Model 3 - Development of transition element between 2D ESL (HOST12) and 3D mixed LW model

Compatibility between two differently modelled sub-domains (by using Model 1 and Model 2) is enforced by degenerating a continuum 3D element through kinematic constraints compatible with deformations predicted by 2D element.

A 3D-to-2D transition element has one or two faces of a 3D element that are kinematically restrained to enforce compatibility with adjacent 2D elements. Such a face is denoted as a transition face in the sequel. The 3D element on the transition face needs to be conditioned for compatibility with DOF of the ESL (HOST12) element to ensure continuity of the combined model. Such an element acts as a transition element to connect two independently modelled sub-domains. Transition is achieved by placing a stack of such transition elements used in different layers of a laminate at the transition face.

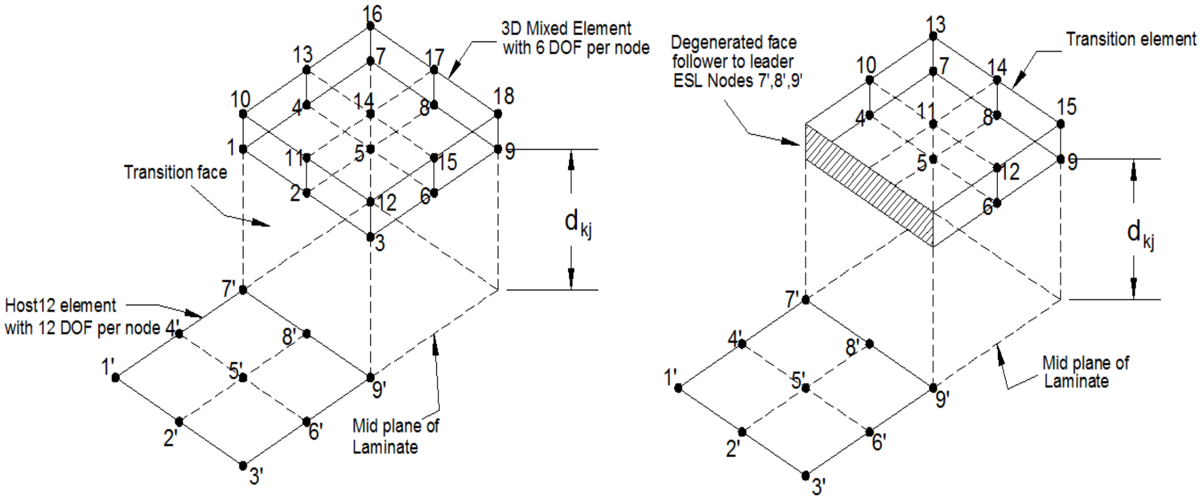

Fig. 1 (a) Configuration of connection between 3D elements and HOST12 elements, and (b) Illustration of degenerated face of the 3D element

A pair of incompatible mesh formulations is shown in Fig. 1(a) wherein a nine node ESL element with twelve DOF per node (node numbers denoted with a prime) is connected to a stack of 3D mixed elements with six DOF per node (three translations and three transverse stresses). Fig. 1(b) shows diagrammatic representation of the transition element with the degenerated transition face. Differently modelled meshes meeting at the transition face represent the same laminate configuration and thickness.

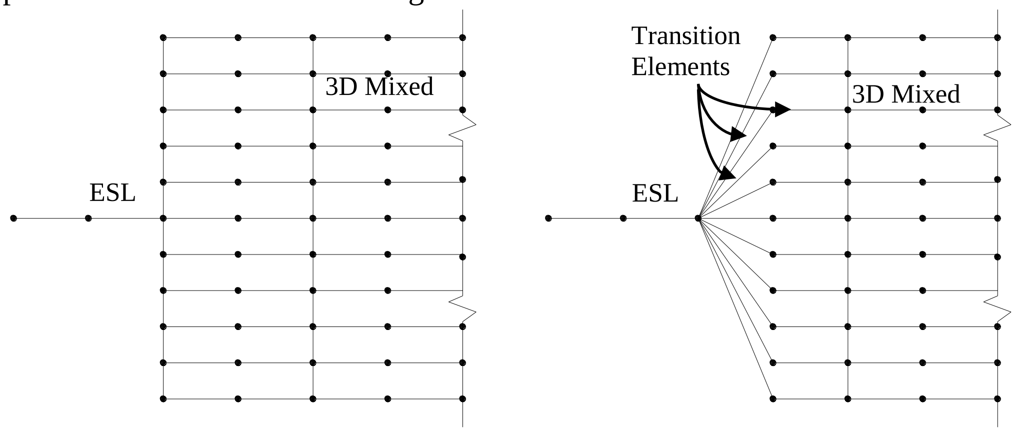

(a) (b)

Fig. 2 An indicative impression of unidirectional transition (a) before implementation of restraint; and (b) after implementation of restraint

Kinematics of any point at a distance ‘d_{kj}’ from the reference plane of the laminate on the transition face is completely described by displacement field for the ESL. Because 2D elements and stack of 3D elements represent the same laminate, motion of the corner 3D node (node 1) (refer Fig. 1(a)) is entirely prescribed by the three translations, three rotations and the higher order terms of its corresponding ESL node (node 7’). Consequently, the DOF associated with nodes 1,2,3,10,11 and 12 are followers to the DOF associated with ESL leader nodes 7’, 8’ and 9’, and hence must be restrained. A transition element is shown in Fig.1(b), where kinematic restraint is imposed on the hatched surface. Three nodes of the ESL on the transition face form 3D elements' transition edge. This edge represents transition face of 3D element stack. An indicative impression of the change in configuration of the 3D element on imposition of the restraint is shown in Fig. 2.

By using displacement field of HOST12 in Eq. (1), kinematics $\{\hat{q}\}^k_{3D}$ of any ‘kth’ node of 3D element on the transition face and corresponding to the ESL leader ‘jth’ node can be completely prescribed as

$$\{\hat{q}\}^k_{3D} = \begin{Bmatrix} u \\ \hat{v} \\ w \end{Bmatrix}^k_{3D} = \begin{bmatrix} 1 & 0 & 0 & d_{kj} & 0 & 0 & d_{kj}^2 & 0 & 0 & d_{kj}^3 & 0 & 0 \\ 0 & 1 & 0 & 0 & d_{kj} & 0 & 0 & d_{kj}^2 & 0 & 0 & d_{kj}^3 & 0 \\ 0 & 0 & 1 & 0 & 0 & d_{kj} & 0 & 0 & d_{kj}^2 & 0 & 0 & d_{kj}^3 \end{bmatrix} \{q\}^j_{2D}$$

$$where\ \{q\}_{2D} = \begin{bmatrix} u_0 & v_0 & w_0 & \theta_x & \theta_y & \theta_z & u_0^* & v_0^* & w_0^* & \theta_x^* & \theta_y^* & \theta_z^* \end{bmatrix}^T \tag{4}$$

or

$$\{\hat{q}\}^k_{3D} = [R]_{kj} \{q\}^j_{2D} \tag{5}$$

By developing the restraint sub-matrices $[R]_{kj}$ for all pairs of 2D and 3D nodes, the transformation matrix [R] for the entire element can be formulated by appropriately populating sub-matrices $[R]_{kj}$ corresponding to every pair. Finite element stiffness property, mass/inertia property matrices and internal force/influence vector for the transition element are obtained by matrix transformations using the constructed corresponding matrices of 3D element and associated transformation matrix as follows,

$$\left.\begin{aligned} [K_e]_{Tr} &= [R]^T [K_e]_{3D} [R] \\ \{F_e\}_{Tr} &= [R]^T \{F\}_{3D} \\ [M_e]_{Tr} &= [R]^T [M_e]_{3D} [R] \end{aligned}\right\} \tag{6}$$

The transformation in Eq. (6) degenerates the transition face of the 3D element which becomes follower to the corresponding HOST12 leader nodes. All elements in the interior of the local transition face are 18 node elements with all nodes modelled using mixed formulation. Stress DOF at the 3D nodes on the transition face are condensed prior to imposition of the restraint. By considering stiffness and mass matrices of the ESL elements, transition elements and the interior LW mixed elements, the global matrices are obtained in the following form after assembly.

$$\begin{aligned} [K]^G &= \sum_{i=1}^{m} \left[K_e^i\right] + \sum_{j=1}^{n} \left[K_e^j\right]_{Tr} + \sum_{l=1}^{k} \left[K_e^l\right] \\ [M]^G &= \sum_{i=1}^{m} \left[M_e^i\right] + \sum_{j=1}^{n} \left[M_e^j\right]_{Tr} + \sum_{l=1}^{k} \left[M_e^l\right] \\ \{F\}^G &= \sum_{i=1}^{m} \left\{F_e^i\right\} + \sum_{j=1}^{n} \left\{F_e^j\right\}_{Tr} + \sum_{l=1}^{k} \left\{F_e^l\right\} \end{aligned} \tag{7}$$

Here

$[K]^G$, $[M]^G$ and $\{F\}^G$ are the global stiffness property matrix, inertia property matrix and nodal influence vector, respectively;

$\left[K_e^i\right]$, $\left[M_e^i\right]$ and $\left\{F_e^i\right\}$ are the element property matrix, inertia property matrix and the element influence vector of i^{th} element, respectively, formed by using mixed LWT;

$\left[K_e^j\right]_{Tr}$, $\left[M_e^j\right]_{Tr}$ and $\left\{F_e^j\right\}_{Tr}$ are the element property matrix, inertia property matrix and element influence vector of j^{th} transition element, respectively; and

$\left[K_e^l\right]$, $\left[M_e^l\right]$ and $\left\{F_e^l\right\}$ are the element stiffness matrix, mass matrix and element nodal load vector of l^{th} ESL element, respectively.

m, *n* and *k* in Eq. (7) represent number of mixed LW, transition and ESL elements.

The displacement vector $\left\{\hat{q}\right\}_{Tr}$ of a transition element is composed of DOF of ESL nodes on the transition edge, and DOF of 3D nodes on the other faces.

The transition element developed by the application of the restraints consists of 108 DOF and 15 nodes for unidirectional transition and a corner element with two adjacent transition edges has 13 nodes and 108 DOF. Such a corner element is developed by applying the kinematic restraint on two adjacent faces.

3.0 Numerical examples

To study 3D state of stresses in the free edge regions, a laminate is modelled by using 3D mixed LW elements at free edge and higher order ESL in remaining part to reduce computational effort. Both models are implemented simultaneously and compatibility between subdomains is established by introducing transition elements. Examples of symmetrical cross ply laminates under in-plane unidirectional strain and transverse doubly sinusoidal load are considered for illustration. Plate under transverse load is considered to be simply supported on all four edges. Substantial reduction in computational effort is achieved as compared to a complete LW mixed FE solution.

3.1 Example 1: Free edge stress analysis of a symmetric cross ply laminate

A symmetric (0/90/90/0) cross ply laminate is considered for free edge stress analysis under action of uniform uniaxial in-plane strain. Width of laminate ‘2*b*’ is considered as ‘4*h*’ and length of laminate ‘*l*’ is taken as ‘10*h*’, where ‘*h*’ is thickness of laminate. Material of laminae is assumed to possess following properties.
E_1 = 138.00GPa; $E_2 = E_3$ = 9.66 GPa; $G_{12} = G_{13}$ = 5.52 GPa;
G_{23} = 4.14 GPa; $\nu_{12} = \nu_{13} = \nu_{23}$ = 0.21;

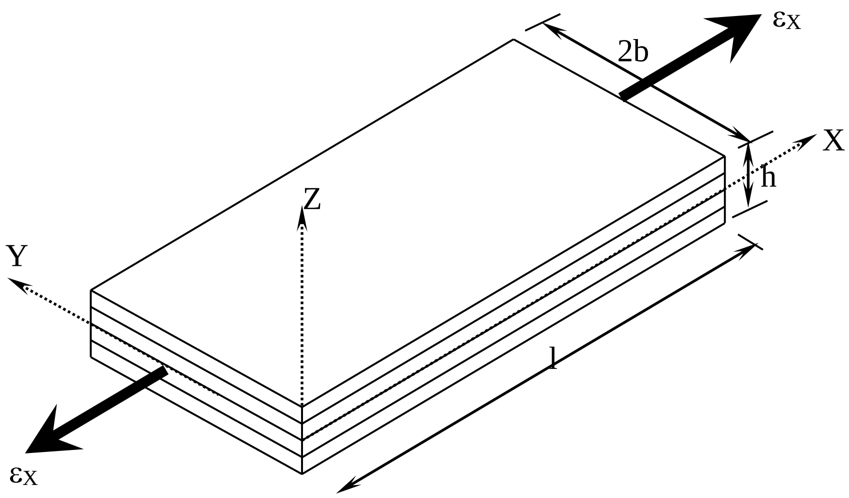

Fig 3 Typical laminate and coordinate axes

Uniform in-plane strain $(\varepsilon_x = 1X10^{-6})$ is introduced along the length of laminate. Implementation of this novel multi-model finite element mesh is done on a quarter part of the laminate. Advantage of symmetry in configuration is taken in implementation of the multi-model FE scheme for a finer discretization. A typical laminate with coordinate axes is shown in Fig 3. Laminate is restrained against deformations along *X* axis at *X=l/2*. A uniform strain is introduced at *X=0*.

Zone in vicinity of *X=0* over entire half width is modelled using a stack of 3D mixed LW elements and in remaining part, higher order ESL (HOST12) is used. Length of local zone (3D mixed LW zone) is taken equal to thickness of laminate. This amounts to about 10% of entire domain of plate. Laminate is discretized using 7 elements along the length and 8 elements along width. A strip of 1 element at free edge along the width is modelled by 3D mixed LW elements. Each layer of laminate is subdivided in 4 sub-layers to accommodate 16 LW mixed 3D elements over the thickness at local free zone. Hence, a total of 176 elements are employed over the domain of laminate. Composition of these elements comprises of 56 ESL and 128 3D mixed LW elements.

Variation of the transverse normal stress at free edge (*X=0*), along the half width of plate is obtained by present multi-model approach. Variation of the transverse normal stress at mid-plane (90-90 interface) and at (90-0) interface are presented in Fig 4 and Fig 5, respectively. Variation of the transverse shear stress (τ_{yz}) at (90-0) interface along the width at free edge is shown in Fig 6.

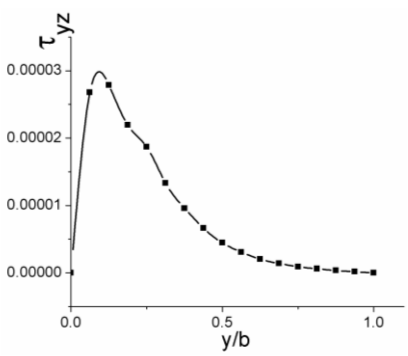

Fig 4 Width wise variation of σ_z on free edge at *X=0* at mid-plane

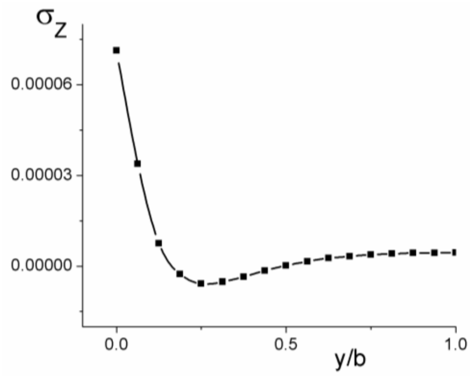

Fig 5 Width wise variation of $\overline{\tau}_{yz}$ at free edge at *X=0* at mid-plane

It is observed that the transverse stresses at the free edge are correctly estimated by the present multi-model approach. Steep stress gradient is predicted at free edge. At the same time, a substantial reduction in computational effort is also achieved. Saving in computational effort as compared to complete 3D mixed LW model can be appreciated. For a complete 3D solution with same mesh discretization, a total of 896 elements would have been required. Reduction in number of elements required to map the domain leads to reduction of DOF and therefore, the computational effort.

3.2 Example 2: Complete stress analysis of a square simply supported sandwich plate under bi-directional sinusoidal transverse load (Core=0.8h)

A (0°/core/0°) square sandwich plate (*l*=2b) under bi-directional sinusoidal transverse load is considered for in-plane as well as inter-laminar stresses. The plate is simply supported on all four edges. The thickness of each face sheet is one tenth of total thickness of sandwich plate. Determination of in-plane and the transverse stresses is accomplished using present combined model. To capture (τ_{yz}), a stack of 3D mixed LW elements are placed at and in vicinity of $(\frac{l}{2},0)$ and remaining laminate is modelled using HOST12 elements. To capture (τ_{xz}), a stack of 3D mixed LW elements are placed at and in vicinity of $(0,b)$ and remaining laminate is modelled using HOST12 elements. For obtaining (σ_z), a stack of 3D mixed LW elements are placed at and in vicinity of $(\frac{l}{2},b)$ and remaining laminate is modelled using HOST12 elements. Material properties and normalization factors used for the analysis are mentioned alongside Table 1. Results for aspect ratios *S*=*l*/*h*= 2, 4, 10, and 20 have been compared in Table 1 with elasticity solution given by Pagano (1970) [11], FE solution by Ramtekkar, Desai (2003) [12] as well as the analytical and finite element solutions presented by various authors. Through thickness variations of the normalized transverse shear stress components and transverse normal stress for the plate with aspect ratio *S* = 4 have been presented in Fig. 7(a-c). Results are in close proximity of exact elasticity solution obtained by Pagano (1970) [11], FE solution by Ramtekkar, Desai (2003) [12]. The agreement of the results with the elasticity solution and 3D fully mixed formulation clearly suggests that such problems can be analyzed with good accuracy by using the present formulation. A substantial reduction in DOF and effort as compared to complete mixed LW solution is observed.

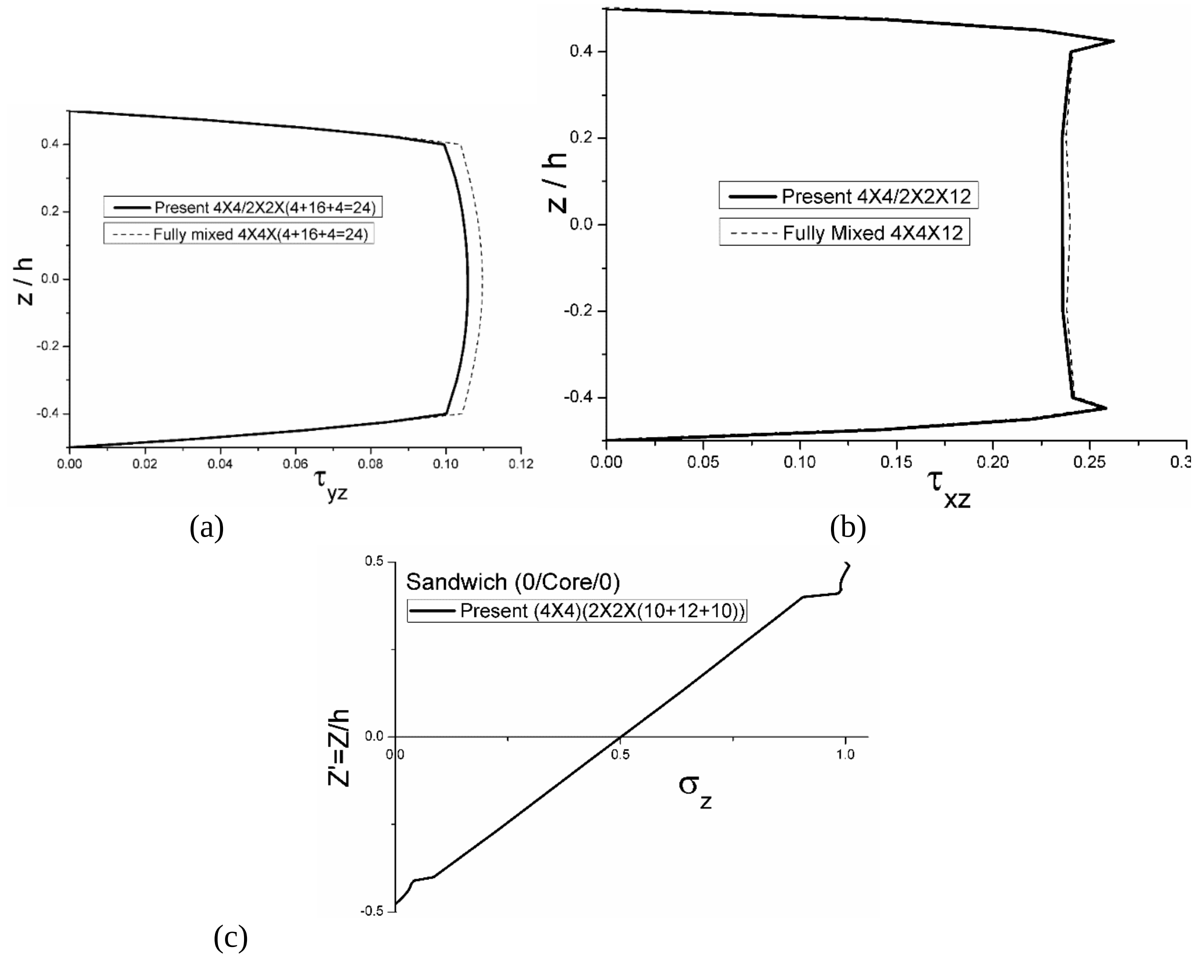

Fig 7 Through thickness variation of a) $\overline{\tau}_{yz}$ **, b)** $\overline{\tau}_{xz}$ **and c)** σ_z

Table 1 **Maximum stresses in square sandwich plate under bi-directional sinusoidal transverse load (Core=0.8h)**

$(FaceSheet: E_1 = 172.4 GPa, E_2 = E_3 = 6.89 GPa, G_{12} = G_{13} = 3.45 GPa, G_{23} = 1.378 GPa, \nu_{12} = \nu_{13} = \nu_{23} = 0.25;$

$Core: E_1 = E_2 = 0.276 GPa, E_3 = 3.45 GPa, G_{12} = 0.1104 GPa, G_{13} = G_{23} = 0.414 GPa, \nu_{12} = \nu_{31} = \nu_{32} = 0.25)$

$$\overline{W} = w\,\frac{100E_2h^3}{q_0a^4},\ \left(\bar{\sigma}_X, \bar{\sigma}_Y, \bar{\tau}_{XY}\right) = \frac{\left(\sigma_X, \sigma_Y, \tau_{XY}\right)h^2}{q_0a^2},\ \left(\bar{\tau}_{XZ}, \bar{\tau}_{YZ}\right) = \frac{\left(\tau_{XZ}, \tau_{YZ}\right)h}{q_0a}$$

S		Source	$\bar{\sigma}_X\,(\frac{a}{2},\frac{b}{2},\pm\frac{h}{2})$		$\bar{\sigma}_Y\,(\frac{a}{2},\frac{b}{2},\pm\frac{h}{2})$		$\bar{\tau}_{XZ}\,(0,\frac{b}{2},0)$	$\bar{\tau}_{YZ}\,(\frac{a}{2},0,0)$	$\bar{\tau}_{XY}\,(0,0,\pm\frac{h}{2})$	
2	i.	Pagano (1970b) [11]	3.278	-2.653	0.452	0.392	0.185	0.142	-0.240	0.234
	ii.	Present	3.1225	-2.516	0.468	-0.417	0.183	0.136	-0.2328	0.2295
4	i.	Pagano (1970b) [11]	1.556	-1.512	0.259	-0.253	0.239	0.107	-0.144	0.148
	ii.	Present	1.501	-1.460	0.267	-0.263	0.2388	0.1055	-0.1424	0.1474
	iii.	Pandya and Kant (1988) [13]	1.523	-	0.241	-	0.275	-	-0.142	-
	iv.	Reddy and Chao (1981) [14]	0.865	-	0.151	-	0.099	-	-0.088	-
	v.	Wu and Lin (1993) [15]	1.548	-	0.241	-	0.249	-	-0.134	-
	vi.	Ramtekkar, Desai (2003) [12]	1.570	-1.524	0.260	-0.255	0.240	0.108	-0.145	0.149
10	i.	Pagano (1970b) [11]	1.153	-1.152	0.110	-0.110	0.300	0.053	-0.071	0.072
	ii.	Present	1.146	-1.145	0.113	-0.113	**0.306**	**0.058**	-.0707	0.0718
	iii.	Pandya and Kant (1988) [13]	1.166	-	0.105	-	0.340	-	-0.069	-
	iv.	Reddy and Chao (1981) [14]	1.015	-	0.077	-	0.111	-	-0.053	-
	v.	Wu and Lin (1993) [15]	1.210	-	0.111	-	0.324	-	-0.071	-
	vi.	Ramtekkar, Desai (2003) [12]	1.159	-1.158	0.111	-0.110	0.303	0.055	-0.071	0.072
20	i.	Pagano (1970b) [11]	±1.110		±0.070		0.317	0.036	$\mp$ 0.051	
	ii.	Present	±1.115		±0.0729		**0.335**	**0.048**	-0.0512	0.0515
	iii.	Present (8X8)/(2X2X16)	±1.106		±0.0713		**0.3216**	**0.0393**	-0.0506	0.0503
	iv.	Wu and Lin (1993) [15]	1.173		0.072		0.353	-	0.052	
	v.	Ramtekkar, Desai (2003) [12]	±1.115		±0.070		0.317	0.036	$\mp$ 0.051	

4.0 Conclusions

A multi-model FE approach is developed for stress analysis of composite laminates. An unique transition element is developed for appropriate compatibility between higher order ESL and 3D mixed LW formulation. The present multi-model approach has been tested over a laminate under uniaxial strain. Results for a transversely loaded simply supported sandwich are also presented. Results obtained through This approach enables mapping of the domain of a laminate with reduced numbers of DOF as compared to any 3D solution. At the same time, accuracy in prediction of inter-laminar stresses at critical zones is also achieved. Reduction in number of DOF renders the methodology a computationally economical.

References

[1] Pipes, R.B. and N. Pagano, Interlaminar stresses in composite laminates under uniform axial extension. Journal of Composite Materials, 1970. 4(4): p. 538-548.

[2] Wang, A. and F.W. Crossman, Some new results on edge effect in symmetric composite laminates. Journal of Composite Materials, 1977. 11(1): p. 92-106.

[3] Pagano, N. and R.B. Pipes, The influence of stacking sequence on laminate strength. Journal of Composite Materials, 1971. 5(1): p. 50-57.

[4] Rybicki, E., Approximate Three-Dimensional Solutions for Symmetric Laminates Under Inplane Loading*. Journal of Composite Materials, 1971. 5(3): p. 354-360.

[5] Wu, C.-P. and C.-S. Hsu, A new local high-order laminate theory. Composite Structures, 1993. 25(1): p. 439-448.

[6] Flesher, N.D. and C.T. Herakovich, Predicting delamination in composite structures. Composites science and technology, 2006. 66(6): p. 745-754.

[7] Shi, Y.-B. and H.-R. Chen, A mixed finite element for interlaminar stress computation. Composite structures, 1992. 20(3): p. 127-136.

[8] Chorng-Fuh, L. and J. Horng-Shian, A new finite element formulation for interlaminar stress analysis. Computers & structures, 1993. 48(1): p. 135-139.

[9] Kant, T. and K. Swaminathan, Analytical solutions for the static analysis of laminated composite and sandwich plates based on a higher order refined theory. Composite structures, 2002. 56(4): p. 329-344.

[10] Ramtekkar, G., Y. Desai, and A. Shah, Mixed finite-element model for thick composite laminated plates. Mechanics of Advanced Materials and Structures, 2002. 9(2): p. 133-156.

[11] Pagano, N., Exact solutions for rectangular bidirectional composites and sandwich plates. Journal of composite materials, 1970b. 4(1): p. 20-34.

[12] Ramtekkar, G., Y. Desai, and A. Shah, Application of a three-dimensional mixed finite element model to the flexure of sandwich plate. Computers & structures, 2003. 81(22): p. 2183-2198.

[13] Pandya, B. and T. Kant, Higher-order shear deformable theories for flexure of sandwich plates-finite element evaluations. International Journal of Solids and Structures, 1988. 24(12): p. 1267-1286.

[14] Reddy, J. and W. Chao, A comparison of closed-form and finite-element solutions of thick laminated anisotropic rectangular plates. Nuclear Engineering and Design, 1981. 64(2): p. 153-167.

[15] Wu, C.-P. and C.-C. Lin, Analysis of sandwich plates using a mixed finite element. Composite Structures, 1993. 25(1): p. 397-405.